

UC Berkeley

UC Berkeley Previously Published Works

Title

Self-regulated growth of LaVO₃ thin films by hybrid molecular beam epitaxy

Permalink

<https://escholarship.org/uc/item/1xs0b7sf>

Journal

Applied Physics Letters, 106(23)

ISSN

0003-6951

Authors

Zhang, Hai-Tian
Dedon, Liv R
Martin, Lane W
[et al.](#)

Publication Date

2015-06-08

DOI

10.1063/1.4922213

Peer reviewed

Self-regulated growth of LaVO₃ thin films by hybrid molecular beam epitaxy

Hai-Tian Zhang, Liv R. Dedon, Lane W. Martin, and Roman Engel-Herbert

Citation: *Applied Physics Letters* **106**, 233102 (2015); doi: 10.1063/1.4922213

View online: <http://dx.doi.org/10.1063/1.4922213>

View Table of Contents: <http://scitation.aip.org/content/aip/journal/apl/106/23?ver=pdfcov>

Published by the [AIP Publishing](#)

Articles you may be interested in

[Growth of SrVO₃ thin films by hybrid molecular beam epitaxy](#)

J. Vac. Sci. Technol. A **33**, 061504 (2015); 10.1116/1.4927439

[Surface composition of BaTiO₃ / SrTiO₃ \(001\) films grown by atomic oxygen plasma assisted molecular beam epitaxy](#)

J. Appl. Phys. **112**, 114116 (2012); 10.1063/1.4768469

[LaCrO₃ heteroepitaxy on SrTiO₃\(001\) by molecular beam epitaxy](#)

Appl. Phys. Lett. **99**, 061904 (2011); 10.1063/1.3624473

[Epitaxially stabilized growth of orthorhombic Lu Sc O₃ thin films](#)

Appl. Phys. Lett. **90**, 192901 (2007); 10.1063/1.2737136

[Structural properties of slightly off-stoichiometric homoepitaxial SrTi_xO_{3-δ} thin films](#)

J. Appl. Phys. **88**, 1844 (2000); 10.1063/1.1305827



Self-regulated growth of LaVO₃ thin films by hybrid molecular beam epitaxy

Hai-Tian Zhang,¹ Liv R. Dedon,^{2,3} Lane W. Martin,^{2,3} and Roman Engel-Herbert^{1,a)}

¹*Department of Materials Science and Engineering and Materials Research Institute, Pennsylvania State University, University Park, Pennsylvania 16802, USA*

²*Department of Materials Science and Engineering, University of California, Berkeley, California 94720, USA*

³*Materials Science Division, Lawrence Berkeley National Laboratory, Berkeley, California 94720, USA*

(Received 2 March 2015; accepted 26 May 2015; published online 8 June 2015)

LaVO₃ thin films were grown on SrTiO₃ (001) by hybrid molecular beam epitaxy. A volatile metalorganic precursor, vanadium oxytriisopropoxide (VTIP), and elemental La were co-supplied in the presence of a molecular oxygen flux. By keeping the La flux fixed and varying the VTIP flux, stoichiometric LaVO₃ films were obtained for a range of cation flux ratios, indicating the presence of a self-regulated growth window. Films grown under stoichiometric conditions were found to have the largest lattice parameter, which decreased monotonically with increasing amounts of excess La or V. Energy dispersive X-ray spectroscopy and Rutherford backscattering measurements were carried out to confirm film compositions. Stoichiometric growth of complex vanadate thin films independent of cation flux ratios expands upon the previously reported self-regulated growth of perovskite titanates using hybrid molecular beam epitaxy, thus demonstrating the general applicability of this growth approach to other complex oxide materials, where a precise control over film stoichiometry is demanded by the application. © 2015 AIP Publishing LLC.

[<http://dx.doi.org/10.1063/1.4922213>]

Materials exhibiting strong electron correlation have stimulated much research interest due to their exotic properties and potential applications in novel electronic devices. Two remarkable examples are the discoveries of high temperature superconductivity¹ and colossal magnetoresistance.² Recently, the interfaces of correlated materials have drawn much attention. New phenomena not observed in their bulk counterparts have been discovered, attributed to the electronic reconstructions that occur at polar/nonpolar interfaces³ to compensate the charge discontinuity, such as in the case of LaVO₃/SrTiO₃,⁴ valence state redistribution across polar interfaces, such as LaVO₃/LaAlO₃,⁵ as well as charge-stabilization of non-bulk-like phases formed at the interfaces between LaVO₃ and LaVO₄.⁶

Detailed growth studies of complex perovskite oxide thin films prepared by pulsed laser deposition (PLD),^{7–9} molecular beam epitaxy (MBE),¹⁰ sputtering,¹¹ and supporting first-principle calculations¹² have shown that the cation stoichiometry can dramatically impact the interface reconstructions. Therefore, the growth of correlated materials with excellent stoichiometry control is of critical importance to gain further insights into the intrinsic optoelectronic properties of these materials and ultimately their heterostructures. In conventional MBE, one way to ensure excellent thin film stoichiometry is by employing an adsorption controlled growth, where the constituents forming the film are supplied to the sample with the volatile component in excess. For a proper choice of growth rate and temperature, excess amounts of volatile species accumulating on the growing surface can re-evaporate instead of getting incorporated into the film. This approach has been successfully employed for

the growth of compound semiconductors^{13–15} and has been applied to the growth of complex oxides BiFeO₃,¹⁶ PbTiO₃,¹⁷ and BiMnO₃¹⁸ as well. However, since the Mott insulator LaVO₃ does not contain any volatile constituent, such as bismuth oxide or lead oxide, but only low vapour pressure components, a self-regulated approach seems to be not feasible.

As a complementary approach to conventional MBE, hybrid MBE has been previously employed to grow SrTiO₃^{19,20} and GdTiO₃²¹ in a self-regulated manner, provided that growth temperatures were high enough. Furthermore, the precise control over the stoichiometry of NdTiO₃ thin films²² has been demonstrated as well. In contrast to conventional MBE, where elements are supplied through thermal evaporation from effusion cells and are oxidized at the sample surface by exposure to either molecular oxygen, oxygen plasma, or ozone, in hybrid MBE one of the cations—the transition metal element titanium—is supplied using the metal-organic precursor—titanium tetra-isopropoxide (TTIP). This approach to utilize a volatile precursor, in which Ti is coordinated by 4 oxygen, not only allowed for growth rates much higher than normally achieved from fluxes of elemental Ti²³ generated by high temperature effusion cells^{24,25} or sublimation sources²⁶ but also enabled the growth in a self-regulated manner, which was attributed to the volatility of the metalorganic precursor TTIP.¹⁹ Moreover, high-quality SrTiO₃ films were grown directly on silicon using this technique.²⁷

Here, we expand this growth approach towards other transition metal elements by using vanadium-oxy-triisopropoxide (VTIP) as a precursor to demonstrate the generalizability of this approach in material systems other than the titanates. We show that the self-regulated growth window of the Mott insulator LaVO₃ can be accessed by co-supplying

^{a)}Electronic mail: rue2@psu.edu

La metal from an effusion cell and the metal organic precursor VTIP in the presence of molecular oxygen.

Heteroepitaxial growth was carried out in a DCA M600 MBE reactor with a base pressure of 5×10^{-10} Torr. Growth of LaVO_3 thin films was carried out on SrTiO_3 (100) substrates (MTI Corporation). Before growth, substrates were cleaned in an ultrasonic bath of acetone and isopropanol, loaded into the system, and baked for 3 h at 150°C in the load lock, followed by an anneal in a remote oxygen plasma (RF plasma power 250 W) for 20 min at 800°C in the growth chamber. The metalorganic precursor VTIP (vacuum distilled, trace metal impurity 4N, MULTIVALENT Laboratory) was supplied via a heated gas inlet system connected to a gas injector without using an additional carrier gas. A variable leak valve in combination with a capacitance manometer was used to precisely regulate and maintain a constant gas inlet pressure (VTIP pressure) and thus VTIP flux. Lanthanum (4N, Ames National Lab) was supplied by thermal evaporation from a high temperature effusion cell. A series of LaVO_3 thin films were grown on SrTiO_3 (100) for varying VTIP gas inlet pressures ranging from 25 to 50 mTorr. The La flux was fixed at $2.0 \times 10^{13}/\text{cm}^2 \text{ s}^{-1}$ for all samples grown, which was calibrated using a quartz crystal microbalance. A nominal La flux stability of 0.3% was determined from film thickness variation and will be discussed later. Film growth was performed at a sample temperature of 800°C (substrate heater thermocouple). La and VTIP were co-supplied for 60 min in a background pressure of 1×10^{-7} Torr of molecular oxygen supplied through an RF plasma source (turned off during the growth) pointed at the sample. The growth was characterized *in-situ* using reflection high energy electron diffraction (RHEED). High-resolution X-ray diffraction (XRD) was carried out using a Phillips X'Pert Panalytical MRD Pro thin film diffractometer equipped with a duMond–Hart–Partels Ge (440) incident beam monochromator and $\text{Cu K}\alpha_1$ radiation. XRD results were fitted and the error of lattice parameter was determined to be $\pm 0.001 \text{ \AA}$.²⁸ A Bruker Dimension Icon atomic force microscope (AFM) was operated in peak force tapping mode to measure the film surface morphology. Film composition was characterized by energy dispersive X-ray spectroscopy (EDS) and Rutherford backscattering (RBS) measurements. EDS was carried out in Nova NanoSEM 630 system with incident electron energy of 5 keV. RBS was performed in Lawrence Berkeley National Laboratory with incident ion energy of 3040 keV, incident angle $\alpha = 22.5^\circ$, exit angle $\beta = 25.35^\circ$, and scattering angle $\theta = 168^\circ$.

High resolution 2θ - ω XRD scans for films grown at different VTIP gas inlet pressures are shown in Fig. 1(a). Except for the film grown at 25 mTorr VTIP, pronounced Kiessig fringes were observed throughout the film series, indicating abrupt interfaces and smooth surfaces. The film peak was independent of VTIP gas inlet pressure in the range between 31 and 33.5 mTorr and was further found to shift to larger 2θ values with increasing difference of VTIP gas inlet pressures from these values, indicating a reduction of the film lattice parameter. Figure 1(b) shows the out-of-plane film lattice parameter a_\perp as a function of VTIP gas inlet pressure, together with V to La ratios extracted from EDS and

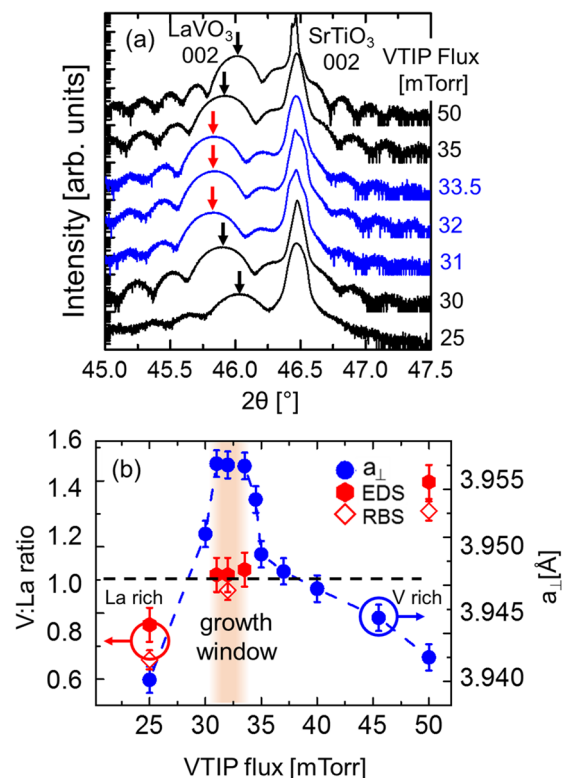


FIG. 1. (a) 2θ - ω X-ray diffraction scans around the SrTiO_3 002 substrate peak. LaVO_3 film peaks are indicated by an arrow. (b) Out-of-plane film lattice parameter a_\perp for LaVO_3 films grown at various La to VTIP flux ratios, extracted from the XRD scans shown in (a). V:La ratios extracted from EDS and RBS measurements along this series were also plotted. The La flux was fixed at $2.0 \times 10^{13} \text{ cm}^{-2} \text{ s}^{-1}$, while the VTIP flux was varied. Stoichiometric growth conditions were found for VTIP gas inlet pressures between 31 and 33.5 mTorr.

RBS measurements. The lattice parameter of stoichiometric LaVO_3 has been previously determined from the bulk (Pbnm).²⁹ Using $a = 5.555 \text{ \AA}$, $b = 5.553 \text{ \AA}$, and $c = 7.848 \text{ \AA}$, a pseudo-cubic lattice parameter of $a_p = 3.926 \text{ \AA}$ was determined for unstrained films. The expansion of the LaVO_3 out-of-plane lattice parameter $a_\perp = 3.956 \text{ \AA}$ shown in Fig. 1(b) was attributed to the biaxial compressive strain (-0.56%) imposed by SrTiO_3 . It is remarkable that unlike in the well-studied case of SrTiO_3 ,^{30–32} and also in the case of SrVO_3 ,³³ where the lattice parameter monotonically expands with increasing amounts of cation non-stoichiometry, the opposite trend was found for LaVO_3 films, in agreement with earlier reports on bulk LaVO_3 .^{29,34}

From Fig. 1(b), it is found that for VTIP fluxes smaller than 31 mTorr and larger than 33.5 mTorr, the out of plane lattice parameter was reduced, indicating a non-stoichiometric film. For VTIP pressures ranging between 31 and 33.5 mTorr, the film lattice parameter was found to be independent of the cation flux ratio, demonstrating the existence of a self-regulated growth window for LaVO_3 . V to La ratios measured in EDS and RBS further confirmed the existence of self-regulated growth window, where the V:La ratios remained close to 1 in this region. The thickness of films grown inside the window was obtained by fitting the periodicity of Kiessig fringes observed in XRD.²⁸ For LaVO_3 grown at 31, 32, and 33.5 mTorr VTIP, all thicknesses were in the range of

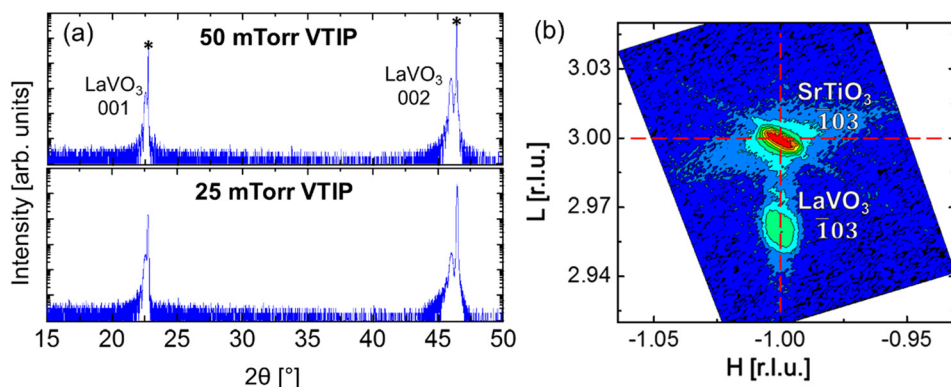


FIG. 2. (a) Wide-range 2θ - ω XRD scans for LaVO_3 films grown at the most V rich (50 mTorr) and most La rich (25 mTorr) condition. SrTiO_3 substrate peaks are denoted with asterisks. (b) Reciprocal space mapping around the $\bar{1}03$ peak of SrTiO_3 (substrate) and LaVO_3 grown inside the growth window ($p_{\text{VTIP}} = 32$ mTorr). The red dotted lines are a guide to the eye.

(37.5 ± 0.1) nm. Assuming that the self-regulated growth is enabled by the volatility of VTIP, a nominal La flux stability of 0.3% can be determined from this film thickness variation, demonstrating an excellent growth-to-growth reproducibility. Films grown at too small VTIP pressures were La-rich, whereas films grown at too high VTIP pressures were V-rich. No secondary phases were found from wide-range XRD scans for films grown at 25 mTorr VTIP (most La-rich growth condition) and 50 mTorr VTIP (most V rich growth condition), see Fig. 2(a). Figure 2(b) shows the reciprocal space map around the $\bar{1}03$ reflections of SrTiO_3 substrate and a LaVO_3 film grown at 32 mTorr VTIP. The stoichiometric LaVO_3 films were coherently strained. Since the film lattice parameter decreased with the increasing level of cation non-stoichiometry, the imposed strain was reduced as well, which further reduced the out-of-plane lattice parameter for non-stoichiometric films.

RHEED was used to monitor the growth *in-situ* and to relate changes in the diffraction pattern to differences in the growth condition,^{20,21,35–37} attempting to reliably predict if the grown film was stoichiometric, and if not, whether La or V was supplied in excess. As shown in Fig. 3, films grown under La-rich conditions showed a spotty RHEED pattern along both the $[100]$ and $[110]$, indicating a crystalline film, but a rough surface, in agreement with the disappearance of the Kiessig fringes in the XRD scans shown in Fig. 1(a). For films grown inside the growth window, streaky RHEED and various weak reflections in addition to the main diffractions spots were found, which was attributed to a smooth surface and the superposition of different surface reconstructions. In particular, a 2×2 and a 3×3 reconstruction pattern was identified along both the $[100]_p$ and $[110]_p$ azimuth. The additional 2×2 reflections could arise either from surface reconstruction or from the lower symmetry of LaVO_3 compared to SrTiO_3 . The orthorhombic distortion and the octahedral tilt present in LaVO_3 ³⁸ result in a doubling of the unit cell compared to SrTiO_3 and additional RHEED reflections between the main diffraction streaks are expected. The superimposed, weak 3×3 pattern was attributed to a reconstructed surface. In contrast, for films grown under V-rich conditions ($p_{\text{VTIP}} = 50$ mTorr), the relatively weak surface reconstruction peaks disappeared and intensity of the diffraction pattern was reduced as well, while the RHEED background intensity increased, which might indicate the presence of a thin, amorphous overlayer. Direct measurements of the film surface

morphology by atomic force microscopy confirmed the trend. Figure 4 shows $2 \times 2 \mu\text{m}^2$ wide scans for films grown under La-rich, stoichiometric, and V-rich conditions. The surface of La-rich film was dominated by small islands of varying heights ranging between 3 and 12 nm. It is speculated that this porous, granular structure might be due to the accumulation of excess La on the surface, which could build up despite the pronounced incorporation of excess La into the film. The root means square (rms) roughness values of these surfaces were quite large (1.52 nm). Films grown in the growth window showed very smooth surfaces with an rms surface roughness of 0.31 nm. An atomic terrace morphology with laterally extended terraces separated by a unit cell step height was not found, which is in contrast to a terrace-like structure reported for LaVO_3 grown by PLD on TiO_2 terminated SrTiO_3 at 600°C .³⁹ To directly prove that the film surface morphology

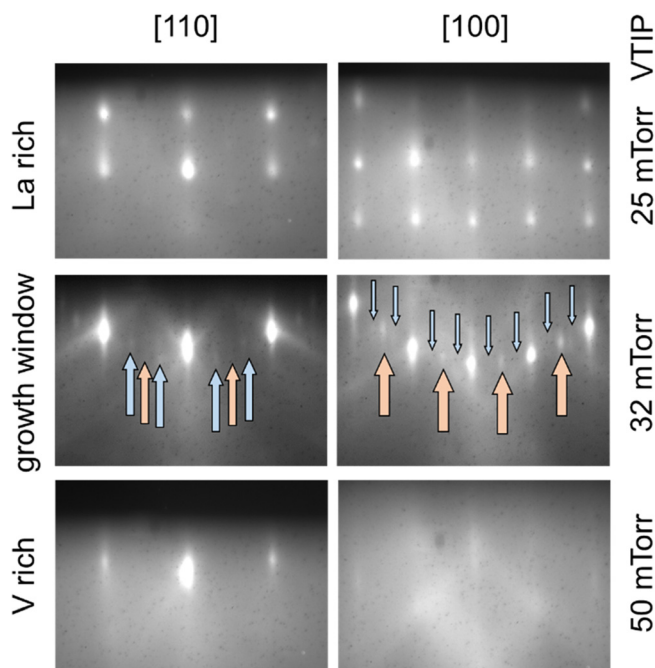


FIG. 3. RHEED pattern of LaVO_3 films grown under La rich (top), stoichiometric (middle), and V rich growth conditions. Diffraction images were captured with the electron beam along the $[110]$ and $[100]$ azimuth after film growth and subsequent cool down to $T_{\text{sub}} = 250^\circ\text{C}$. The red arrows indicate reflections arising from either a 2×2 surface reconstruction or the orthorhombic distortion of LaVO_3 , while the blue arrows indicate reflections attributed to a 3×3 reconstruction.

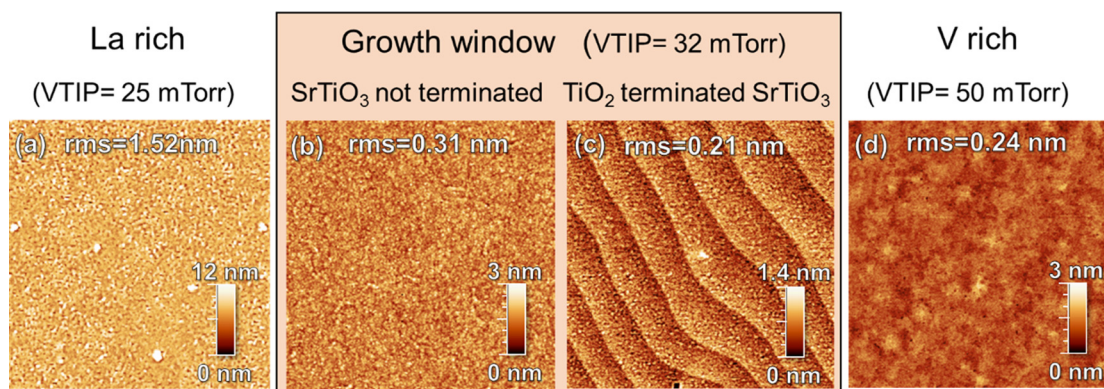


FIG. 4. $2 \times 2 \mu\text{m}^2$ AFM scans of LaVO_3 films grown under (a) La rich condition (25 mTorr), stoichiometric condition (32 mTorr) on (b) un-terminated and (c) TiO_2 -terminated SrTiO_3 substrates, and (d) V rich conditions (50 mTorr).

is determined by the substrate surface preparation and their careful termination, LaVO_3 was grown under stoichiometric condition on TiO_2 -terminated SrTiO_3 . Atomic terrace morphology was observed in this case with an rms roughness of 0.21 nm, see Fig. 4(c). For films grown under V-rich conditions, the film surface remained rather flat as well with an rms values of 0.24 nm, see Fig. 4(d).

In summary we have shown that a self-regulated growth window exists for the growth of LaVO_3 by hybrid MBE. These experimental results indicate the general applicability of this growth approach to enable the synthesis of complex oxide thin films with excellent stoichiometric control. The results exemplify that favourable growth kinetics can be enabled by introducing a volatile metal-organic precursor into the growth process. The existence of self-regulated growth in vanadate and titanate thin films using the hybrid MBE approach allows one to easily maintain stoichiometric conditions throughout oxide heterostructure growth with different transition metals, providing a pathway to separate the intrinsic phenomena emerging at interfaces between conventional band insulator and correlated materials⁴ from extrinsic effects that might be unintentionally introduced during film growth due to limitation in stoichiometry control in other thin film growth techniques.

L.R.D. and L.W.M. acknowledge support from the Department of Energy under Grant No. DE-SC0012375 for RBS measurements and analysis. H.-T. Z. and R. E.-H. acknowledge support from the National Science Foundation through the Penn State MRSEC program DMR-1420620.

¹J. G. Bednorz and K. A. Müller, *Z. Phys. B: Condens. Matter* **64**, 189 (1986).

²A. P. Ramirez, *J. Phys.: Condens. Matter* **9**, 8171 (1997).

³S. Okamoto and A. J. Millis, *Nature* **428**, 630 (2004).

⁴Y. Hotta, T. Susaki, and H. Y. Hwang, *Phys. Rev. Lett.* **99**, 236805 (2007).

⁵M. Takizawa, Y. Hotta, T. Susaki, Y. Ishida, H. Wadati, Y. Takata, K. Horiba, M. Matsunami, S. Shin, M. Yabashi, K. Tamasaku, Y. Nishino, T. Ishikawa, A. Fujimori, and H. Y. Hwang, *Phys. Rev. Lett.* **102**, 236401 (2009).

⁶L. Fitting Kourkoutis, Y. Hotta, T. Susaki, H. Hwang, and D. Muller, *Phys. Rev. Lett.* **97**, 256803 (2006).

⁷E. Breckenfeld, N. Bronn, J. Karthik, A. R. Damodaran, S. Lee, N. Mason, and L. W. Martin, *Phys. Rev. Lett.* **110**, 196804 (2013).

⁸M. Gholikhani, Q. Y. Lei, G. Chen, J. E. Spanier, H. Ghassemi, C. L. Johnson, M. L. Taheri, and X. X. Xi, *J. Appl. Phys.* **114**, 027008 (2013).

⁹H. K. Sato, C. Bell, Y. Hikita, and H. Y. Hwang, *Appl. Phys. Lett.* **102**, 251602 (2013).

¹⁰M. P. Warusawithana, C. Richter, J. A. Mundy, P. Roy, J. Ludwig, S. Paetel, T. Heeg, A. A. Pawlicki, L. F. Kourkoutis, M. Zheng, M. Lee, B. Mulcahy, W. Zander, Y. Zhu, J. Schubert, J. N. Eckstein, D. A. Muller, C. S. Hellberg, J. Mannhart, and D. G. Schlom, *Nat. Commun.* **4**, 2351 (2013).

¹¹I. M. Dildar, D. B. Boltje, M. H. S. Hesselberth, J. Aarts, Q. Xu, H. W. Zandbergen, and S. Harkema, *Appl. Phys. Lett.* **102**, 121601 (2013).

¹²A. Sorokine, D. Bocharov, S. Piskunov, and V. Kashcheyevs, *Phys. Rev. B* **86**, 155410 (2012).

¹³K. G. Gunther, *Z. Naturforsch.* **13**, 1081 (1958).

¹⁴J. R. Arthur, *J. Appl. Phys.* **39**, 4032 (1968).

¹⁵J. Y. Tsao, *Materials Fundamentals of Molecular Beam Epitaxy* (Elsevier, 1992).

¹⁶J. F. Ihlefeld, A. Kumar, V. Gopalan, D. G. Schlom, Y. B. Chen, X. Q. Pan, T. Heeg, J. Schubert, X. Ke, P. Schiffer, J. Orenstein, L. W. Martin, Y. H. Chu, and R. Ramesh, *Appl. Phys. Lett.* **91**, 071922 (2007).

¹⁷C. D. Theis, J. Yeh, D. G. Schlom, M. E. Hawley, and G. W. Brown, *Thin Solid Films* **325**, 107 (1998).

¹⁸J. H. Lee, X. Ke, R. Misra, J. F. Ihlefeld, X. S. Xu, Z. G. Mei, T. Heeg, M. Roeckerath, J. Schubert, Z. K. Liu, J. L. Musfeldt, P. Schiffer, and D. G. Schlom, *Appl. Phys. Lett.* **96**, 262905 (2010).

¹⁹J. Son, P. Moetakef, B. Jalan, O. Bierwagen, N. J. Wright, R. Engel-Herbert, and S. Stemmer, *Nat. Mater.* **9**, 482 (2010).

²⁰A. P. Kajdos and S. Stemmer, *Appl. Phys. Lett.* **105**, 191901 (2014).

²¹P. Moetakef, J. Y. Zhang, S. Raghavan, A. P. Kajdos, and S. Stemmer, *J. Vac. Sci. Technol., A* **31**, 041503 (2013).

²²P. Xu, D. Phelan, J. Seok Jeong, K. Andre Mkhoyan, and B. Jalan, *Appl. Phys. Lett.* **104**, 082109 (2014).

²³B. Jalan, R. Engel-Herbert, N. J. Wright, and S. Stemmer, *J. Vac. Sci. Technol., A* **27**, 461 (2009).

²⁴Z. Yu, Y. Liang, C. Overgaard, X. Hu, J. Curless, H. Li, Y. Wei, B. Craigo, D. Jordan, R. Droopad, J. Finder, K. Eisenbeiser, D. Marshall, K. Moore, J. Kulik, and P. Fejes, *Thin Solid Films* **462–463**, 51 (2004).

²⁵P. Fisher, H. Du, M. Skowronski, P. A. Salvador, O. Maksimov, and X. Weng, *J. Appl. Phys.* **103**, 013519 (2008).

²⁶C. D. Theis, *J. Vac. Sci. Technol., A* **14**, 2677 (1996).

²⁷L. Zhang and R. Engel-Herbert, *Phys. Status Solidi RRL* **8**, 917 (2014).

²⁸J. M. LeBeau, R. Engel-Herbert, B. Jalan, J. Cagnon, P. Moetakef, S. Stemmer, and G. B. Stephenson, *Appl. Phys. Lett.* **95**, 142905 (2009).

²⁹H. Seim and H. Fjellvåg, *Acta Chem. Scand.* **52**, 1096 (1998).

³⁰T. Ohnishi, K. Shibuya, T. Yamamoto, and M. Lippmaa, *J. Appl. Phys.* **103**, 103703 (2008).

³¹B. Jalan, P. Moetakef, and S. Stemmer, *Appl. Phys. Lett.* **95**, 032906 (2009).

³²C. M. Brooks, L. F. Kourkoutis, T. Heeg, J. Schubert, D. A. Muller, and D. G. Schlom, *Appl. Phys. Lett.* **94**, 162905 (2009).

³³J. A. Moyer, C. Eaton, and R. Engel-Herbert, *Adv. Mater.* **25**, 3578 (2013).

³⁴H. Seim, H. Fjellvåg, and B. C. Hauback, *Acta Chem. Scand.* **52**, 1301 (1998).

- ³⁵P. Moetakef, D. G. Ouellette, J. Y. Zhang, T. A. Cain, S. J. Allen, and S. Stemmer, *J. Cryst. Growth* **355**, 166 (2012).
- ³⁶J. H. Haeni, C. D. Theis, and D. G. Schlom, *J. Electroceram.* **4**, 385 (2000).
- ³⁷M. P. Warusawithana, C. Cen, C. R. Slesman, J. C. Woicik, Y. Li, L. F. Kourkoutis, J. A. Klug, H. Li, P. Ryan, L.-P. Wang, M. Bedzyk, D. A. Muller, L.-Q. Chen, J. Levy, and D. G. Schlom, *Science* **324**, 367 (2009).
- ³⁸K. J. Choi, S. H. Baek, H. W. Jang, L. J. Belenky, M. Lyubchenko, and C. B. Eom, *Adv. Mater.* **22**, 759 (2010).
- ³⁹Y. Hotta, Y. Mukunoki, T. Susaki, H. Y. Hwang, L. Fitting, and D. A. Muller, *Appl. Phys. Lett.* **89**, 031918 (2006).